

Formation and direct writing of color centers in LiF using a laser-induced extreme ultraviolet plasma in combination with a Schwarzschild objective

Frank Barkusky, Christian Peth, and Klaus Mann

Laser-Laboratorium Göttingen e.V., Hans-Adolf-Krebs-Weg 1, D-37077 Göttingen, Germany

Torsten Feigl and Norbert Kaiser

Fraunhofer-Institut für Angewandte Optik und Feinmechanik, Albert-Einstein-Strasse 7, D-07745 Jena, Germany

(Received 15 June 2005; accepted 22 August 2005; published online 6 October 2005)

In order to generate high-energy densities of 13.5 nm radiation, an extreme ultraviolet (EUV) Schwarzschild mirror objective with a numerical aperture of 0.44 and a demagnification of 10 was developed and adapted to a compact laser-based EUV source. The annular spherical mirror substrates were coated with Mo/Si multilayer systems. With a single mirror reflectance of more than 65% the total transmittance of the Schwarzschild objective exceeds 40% at 13.5 nm. From the properties of the EUV source (pulse energy 3 mJ at 13.5 nm and plasma diameter approximately 300 μm), energy densities of 73 mJ/cm^2 at a pulse length of 6 ns can be estimated in the image plane of the objective. As a first application, the formation of color centers in lithium fluoride crystals by EUV radiation was investigated. F_2 , F_3 , and F_3^+ color centers could be identified by absorption spectroscopy. The formation dynamics was studied as a function of the EUV dose. By imaging of a pinhole positioned behind the plasma, an EUV spot of 5 μm diameter was generated, which accomplishes direct writing of color centers with micrometer resolution. © 2005 American Institute of Physics. [DOI: 10.1063/1.2072147]

I. INTRODUCTION

Extreme ultraviolet lithography (EUVL) can be regarded as the extension of optical lithography to a shorter wavelength and is one option for the semiconductor industry for next generation lithography (NGL) systems.¹ Using reflective imaging optics on the basis of multilayer mirrors, electronic devices with structure sizes well below 45 nm could be manufactured at a wavelength of 13.5 nm. For industrial lithographic systems EUV radiation with high average power is required, which can be generated either by laser- or discharge-based plasma sources. Such EUV sources and corresponding beam steering optics are currently being developed with tremendous effort.^{2,3}

Besides semiconductor microlithography, there are also other applications of EUV radiation, which can strongly profit from the EUVL source and optics developments. For instance, Baldacchini and co-workers^{4,5} demonstrated the generation of surface-near color centers in LiF crystals positioned in the vicinity of a laser-produced EUV plasma, generated by focusing a large-volume excimer laser (Hercules) on a solid target. Structuring of such color center areas was achieved by use of a contact mask during EUV exposure.⁶ Color centers in LiF can be used in different applications, e.g., as laser-active medium,^{7,8} for data storage,⁹ or as a detector for EUV microscopy.^{4,10}

Another possibility is the modification of polymers using EUV radiation. For polymethylmethacrylate (PMMA) this was demonstrated by Juha *et al.*, who used a contact mask for direct ablation under the influence of an intense EUV

plasma, generated by a high-energy (multi-Joule) laser system.¹¹ The latter application especially requires high EUV pulse energy densities. These can be achieved by positioning the samples close to the EUV plasma, leading, however, to radiation damage or effects caused by unwanted out-of-band radiation.

Alternatively, EUV optical elements can be employed for focusing or demagnification of the plasma. In this article we report on the development of a high-numerical-aperture (NA) Schwarzschild objective, which was adapted to a compact laser-produced EUV plasma source based on a Xe gas target.¹²⁻¹⁴ Imaging of this plasma leads to a high EUV pulse energy density (approximately 73 mJ/cm^2) far away from the source, capable of structuring or modifying materials with micron resolution and simultaneously avoiding sample damage due to the influence of the hot plasma. Together with a description of the design and characterization of the integrated EUV source and optics system, we present first results on the generation of color centers in lithium fluoride crystals. In comparison to the work of Baldacchini and co-workers,^{4,5,10} the color centers were generated by direct writing, using an EUV mirror objective and a sample translation stage, resulting in a more flexible appliance.

II. EXPERIMENTAL SETUP

A. EUV source

The experimental setup consists of a laser-based EUV source¹²⁻¹⁴ and a separate optics chamber adapted to this source (cf. Fig. 1). EUV radiation is generated by focusing a

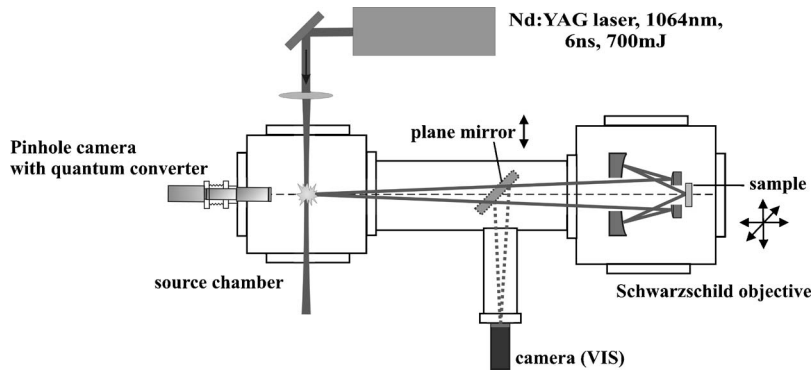


FIG. 1. Schematic drawing of the integrated EUV source and optics system. The sample is mounted on a 3-axes translation stage. Sample adjustment is facilitated by an integrated video camera. Illumination of the sample is realized with a LED (not displayed).

Nd:yttrium aluminum garnet (YAG) laser (fabricated by Inolas, fundamental wavelength 1064 nm, pulse energy 700 mJ, and pulse length 6 ns) into a pulsed gas jet produced by an electromagnetically switched valve. The nozzle tip is located in the center of the vacuum chamber, which is evacuated below 10^{-3} mbars due to the low mean-free path of EUV radiation at atmospheric pressure. Xenon is used as target gas, emitting broadband radiation from 8 to 15 nm.³ The plasma can be monitored with a pinhole camera, consisting of a charge coupled device (CCD) chip with an EUV-to-Visible quantum converter and a pinhole (diameter 30 μm) coated with a zirconium foil (thickness approximately 200 nm) for blocking out-of-band radiation.¹³

Table I shows selected properties of the employed EUV source.

B. Schwarzschild objective

The goal of the designed EUV objective was to achieve a high-energy density in the focus plane, combined with high spatial resolution (several lines per micron) and a compact setup. For the latter reason, no condenser mirror was included in the design of the optical system. The energy density H obtained in the image plane of an aberration-free mirror system can be calculated from

$$H = QR^n \frac{\Omega}{4\pi} \frac{4}{\pi(Md)^2}, \quad (1)$$

where Q is the pulse energy of the plasma in 4π sr, R the reflectance of a single mirror, n the number of reflections, Ω the acceptance solid angle of the objective, M the magnification, and d the diameter of the source. By comparing different mirror configurations with the help of ray-tracing calculations, Schwarzschild mirror systems with two annular spherical mirrors turned out to have optimal optical and mechanical performances with respect to the intended application.

Table II summarizes optical and mechanical dimensions of the mirror design. By inserting these data in Eq. (1), a theoretical energy density of about 73 mJ/cm² can be evalu-

ated for a plasma energy of 3 mJ and a source diameter of 300 μm . A measurement of the EUV pulse energy was performed close to the image plane of the objective, using a differential calorimeter with a sensitivity in the submicrowatt range. After spectral filtering by the Mo/Si multilayer mirrors and additional blocking by a 200 nm Zr foil, an energy signal of approximately 0.7 μJ /pulse was registered, leading to an energy density close to the theoretical value.

In comparison to a classical Schwarzschild objective the annular design offers considerable fabrication advantages. First, both mirrors can be mounted directly at the rim of the substrate, resulting in a more stable adjustment and a less elaborate mirror holder. Second, the variation of the incident angles are small (primary mirror: $4^\circ < \alpha < 10.2^\circ$; secondary mirror: $1.5^\circ < \alpha < 3.8^\circ$), allowing the use of laterally homogeneous Mo/Si multilayer stacks.

To ensure highest thermal stability of the EUV objective low expansion materials were used for both the mirror substrates and the mechanical holder. The mirror substrates are fabricated from ULE (ultralow expansion) titanium silica glass with a thermal expansion coefficient of $0 \pm 3 \times 10^{-8}$ 1/K [5–35 $^\circ\text{C}$, according to manufacturer information (Corning)]. Parts of the mechanical holder system are made of Invar, which has a nearly ten times smaller thermal expansion coefficient than stainless steel.

With regard to an optimum adaptation to the EUV source, the objective was designed with a horizontal optical axis. The resulting deformation of the substrates due to gravity and mechanical-holder-induced forces were simulated with finite element modeling simulations. Computed distortions are in the order of ~ 1 nm, which can be regarded as uncritical for the intended resolution. The mirrors were coated at the Fraunhofer IOF Jena with a Mo/Si multilayer system designed for maximum reflectivity at the operation wavelength of 13.5 nm.¹⁵ The Mo/Si bilayer thickness for both mirrors was optimized for highest reflectivity and is $d = (6.97 \pm 0.2)$ nm for the primary and $d = (6.92 \pm 0.2)$ nm for the secondary mirror. The multilayer was coated with dc magnetron sputtering using the sputtering system “neutral electrode safety system” (NESSY) (developed by Leybold Optics Dresden GmbH). Both the primary and secondary mirror substrates were coated in the same deposition run to ensure an optimum wavelength matching. The measured mirror reflectance ranges from 65.2% to 66.7% at 13.5 nm at the clear aperture and the corresponding angles of incidence.

TABLE I. Source parameters of the laser-based EUV plasma source.

Wavelength (λ)	8–15 nm
Energy (Q)	3 mJ (13.5 nm, 2% BW, 4π)
Plasma diameter (d)	300 μm (FWHM, nearly spherical)
Repetition rate (f_p)	1 Hz

TABLE II. Optical and mechanical dimensions of the EUV mirror objective.

Distance source—image plane	520.5 mm
Magnification (M)	0.102
Numerical aperture (NA)	0.44
Acceptance angle (Ω)	5.33 msr
Reflectivity (R)	$\approx 65\%$ (per mirror)
Number of mirrors (n)	2
Spot size	approximately 30 μm (source image) 5 $\mu\text{m} < d < 30 \mu\text{m}$ (imaging of pinhole)
Energy density (H)	approximately 73 mJ/cm^2 (source image) <73 mJ/cm^2 (imaging of pinhole)

C. Setup

The Schwarzschild objective is positioned in a separate vacuum chamber connected to the source chamber (cf. Fig. 1). The alignment of the mirror objective was performed at atmosphere, using a Hartmann-Shack wave-front sensor in the visible spectral range.^{16,17} For simulation of the EUV plasma, the tip of a fiber-coupled diode laser (LINOS, wavelength $\lambda=639$ nm, fiber core diameter 4 μm) was mounted at the plasma position. The wave-front distribution transmitted through the objective was monitored and optimized with regard to minimum aberrations using the Hartmann-Shack sensor. A residual peak-valley aberration of 0.81λ was measured, which is in very good agreement with the value of 0.79λ calculated from the optical path difference (OPD) of the ideal objective and the irregularity of the mirror surfaces.

For sample adjustment a video camera for visible light is mounted in the same distance to the objective as the source (conjugated planes). In order to switch from EUV exposure to adjustment in the visible spectral range, a plane mirror can be positioned in the beam path between source and optics (cf. Fig. 1). Figure 2 shows a photo of the EUV source with integrated Schwarzschild objective. The dimensions of the entire system including laser, power supplies, gas bottle, and vacuum pump are $100 \times 60 \times 145 \text{ cm}^3$ ($W \times D \times H$).

The objective can be operated in the following two different modes:

- Plasma imaging: The EUV plasma is imaged directly, leading to an energy density of approximately

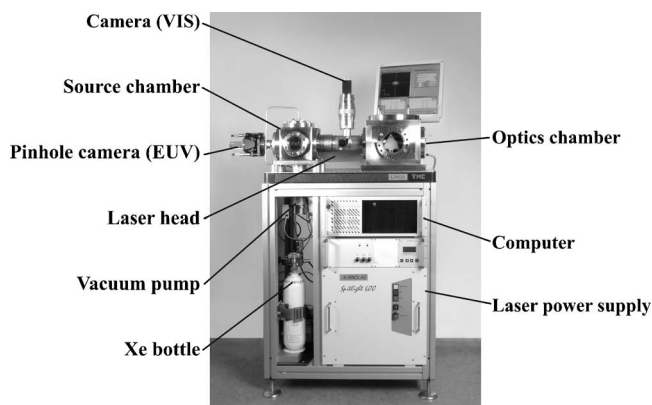


FIG. 2. Photo of the table-top EUV source with integrated Schwarzschild objective.

73 mJ/cm^2 , but a relatively low spatial resolution due to the near-Gaussian intensity distribution of the plasma.¹⁴

- Mask imaging: A pinhole (e.g., 50 μm in diameter) is positioned approximately 5 mm behind the plasma. By translating the sample into the image plane of the pinhole, a writing spot of 5 μm diameter with steep edges is obtained. Ray-tracing simulations show an approximately three times smaller energy density than in the plasma imaging mode due to the reduced fluence on the pinhole.

The objective adjusted in the visible was tested in the EUV spectral range using a knife-edge method, i.e., by moving a razor blade in transverse direction through the image plane. Radiation passing the blade was recorded by an EUV-sensitized CCD camera. Figure 3 (above) shows the integrated intensity measured with this detector as a function of the blade position for the vertical axis of the plasma image.

In the lower diagram the derivative of the smoothed data curve is shown. For comparison, an EUV plasma image was taken by the EUV pinhole camera and scaled down by a factor of 10 (theoretical magnification of the objective). The vertical section of the resulting image (after integrating the intensities over horizontal lines) is also displayed in Fig. 3,

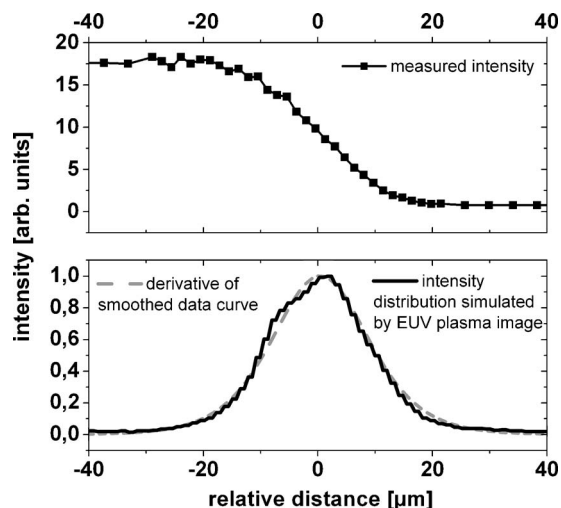


FIG. 3. (Above) EUV knife-edge measurement in the image plane (vertical axis, cf. text); (below) the derivative of the smoothed data corresponds with the ten-times-reduced EUV plasma image as determined with the EUV pinhole camera, yielding a spot diameter of approximately 21 μm (FWHM).

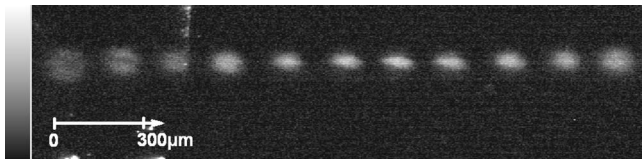


FIG. 4. Color centers generated in LiF, representing EUV intensity distributions at different positions along the optical axis near the image plane. The sample was displaced by $20\ \mu\text{m}$ along the optical axis between two spots. Each spot was generated by a single EUV pulse only. The color centers are visualized by excitation at 248 nm.

indicating excellent agreement with the knife-edge measurement. A vertical spot diameter of approximately $21\ \mu\text{m}$ full width at half maximum (FWHM) can be determined.

III. RESULTS

A. Characterization of color center formation in LiF samples

To study the interaction of high fluence EUV radiation with matter using the mirror objective, lithium fluoride was investigated, which is known as a high-resolution detector for this spectral range.¹⁰ A LiF crystal (Korth Kristalle) was positioned close to the image plane of the objective and exposed to single EUV pulses (Fig. 4). Between two pulses, the sample was displaced by a distance of $20\ \mu\text{m}$ along the optical axis (i.e., through the image plane) and approximately $200\ \mu\text{m}$ laterally (in horizontal direction). The EUV-generated color centers shown in Fig. 4 were excited to fluorescence with a KrF laser at 248 nm immediately after exposure to EUV radiation (according to F color centers, maximum absorption at approximately 250 nm).¹⁸ Since the brightness of the color centers corresponds to the applied EUV fluence, the image plane can be defined properly by this measurement.

In order to identify the generated color centers, spectroscopic measurements were performed on EUV-exposed and unexposed LiF crystals. Figure 5 shows two extinction spectra of LiF samples. The irradiated sample was positioned a distance of 15 mm from the plasma and exposed to 6000 pulses. The spectra were taken with a Lambda 19 spectrometer (Perkin Elmer) immediately after exposure.

The extinction spectrum shows a strong absorption peak at 450 nm, which can be attributed to F_2 and F_3^+ color cen-

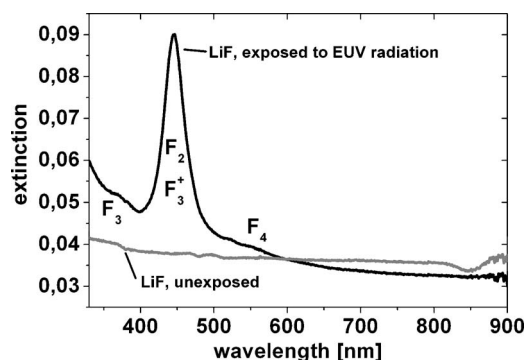


FIG. 5. Extinction spectra of an EUV exposed and an unexposed LiF sample. The absorption peaks correlate well with literature values of color centers (Ref. 18) generated in LiF by gamma radiation.

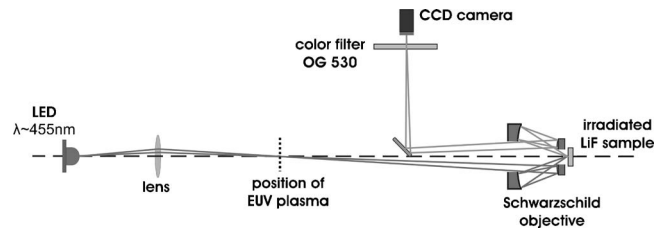


FIG. 6. Schematics setup for generation and *in situ* readout of LiF color centers.

ters. The absorption between 340 and 400 nm is caused by F_3 color centers.¹⁸ Due to the strong absorption at 450 nm, it is possible to employ either an argon-ion laser (457.9 nm) of a laser scanning microscope (Leica) or a blue light-emitting diode (LED) (455 nm) for excitation of the generated color centers.

Figure 6 shows the modified setup for on-line monitoring of generated LiF color centers using a blue LED. The radiation of the LED was imaged both onto the position of the EUV plasma and further, via the mirror objective, onto the sample. The plane mirror was fixed in a position where half of the light coming from the objective was reflected to the camera. This accomplishes simultaneous generation and monitoring of the color centers. For blocking of the excitation wavelength, a color filter (OG530) was integrated.

Using the setup of Fig. 6, the fluorescence signal of generated color centers was recorded as a function of the number of applied EUV pulses for two different LiF crystals (cf. Fig. 7), showing a strong increase in the beginning and a slightly different saturation behavior. Obviously, the first 200 pulses are responsible for nearly one third of the fluorescence measured after 2500 pulses.

After the EUV exposure was terminated, further enhancement of the fluorescence intensity could be observed, as displayed in Fig. 8. The brightness of the color centers increases rapidly during the first two h; after 6 h the intensity is nearly twice as high as directly after exposure, decreasing then slowly until the end of the measurement.

From a comparison with literature data the observed color centers can be attributed to F_3^+ (maximum emission approximately 541 nm)¹⁹ and F_2 (maximum emission approximately 678 nm)¹⁸ centers (belonging to the *M* band),¹⁸ since the blocking filter OG530 transmits radiation with

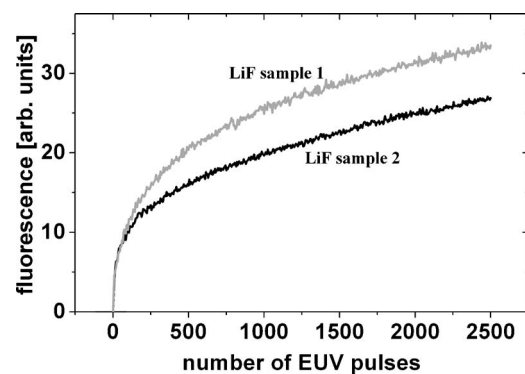


FIG. 7. Increase of fluorescence signal due to F_3^+ and F_2 color center formation as a function of the number of applied EUV pulses (cf. text).

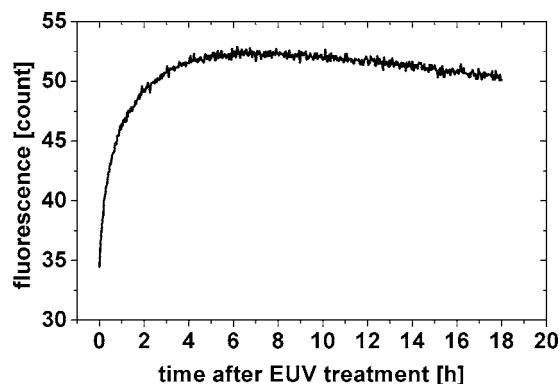


FIG. 8. Fluorescence signal after termination of EUV exposure (cf. text).

wavelengths >530 nm and the CCD camera used as a detector is sensitive below 1000 nm.

The increase of emission intensity can be interpreted by a conversion of different types of color centers. It is known that the concentration of F_2^+ color centers decreases rapidly at room temperature.¹⁸ Since these color centers absorb at a wavelength of 645 nm and are thus not visible with the setup, a neutralization into F_2 centers (absorbing at 455 nm) would lead to an increase of fluorescence energy. Furthermore, a decrease of emission intensity in the M band was observed in combination with a simultaneous increase of F_3^+ color center density during several hours in the dark.²⁰ The observed increase of emission intensity could be of interest in the use of LiF as a detector for short wavelength microscopy. A readout of the samples approximately 6 h after exposure would yield a strongly enhanced contrast.

B. Direct writing of color centers in LiF samples

In order to demonstrate the possibility of direct writing of color centers in LiF, the Schwarzschild objective was used in the mask imaging mode, with a $50\ \mu\text{m}$ pinhole behind the plasma. By translating the sample laterally with a motorized manipulator, letters were written with an EUV spot of about $5\ \mu\text{m}$ diameter (Fig. 9). The sample was moved approximately $3.6\ \mu\text{m}$ between two positions, each site on the sample was exposed to ten EUV pulses. The color centers were visualized with the help of a laser scanning microscope

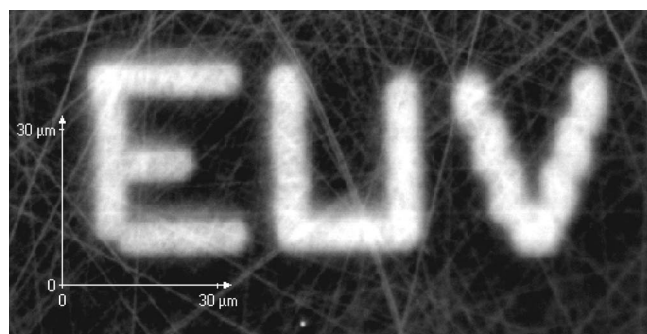


FIG. 9. Direct writing of color centers in LiF, visualized with a laser scanning microscope. The EUV spot has a diameter of $5\ \mu\text{m}$.

(Leica), which uses an argon-ion laser (wavelength 457.9 nm) in fluorescence mode (color filter OG530 in front of the detector).

IV. DISCUSSION

A $10\times$ EUV Schwarzschild objective consisting of two annular spherical mirrors coated with Mo/Si multilayers for 13.5 nm was developed and adapted to a laser-based EUV plasma source. By imaging of the plasma, an EUV spot of $\sim 30\ \mu\text{m}$ diameter at pulse energy densities $>70\ \text{mJ}/\text{cm}^2$ could be generated, as was proven by the knife-edge spot size and calorimetric energy measurements in the image plane. Moreover, a $5\ \mu\text{m}$ spot with steep edges was obtained by projection of a $50\ \mu\text{m}$ pinhole positioned directly behind the plasma. The setup was used to demonstrate direct EUV-induced writing of color centers in LiF crystals, as to our knowledge for the first time by use of a mask imaging technique. The generated color centers could be identified as F_2 , F_3 , and F_3^+ centers by absorption measurements. Using a blue LED for excitation, the formation dynamics could be studied *in situ*, showing an increase of the emission as a function of the number of applied EUV pulses, as well as a further enhancement during the first hours after termination of the EUV irradiation. In order to investigate the interaction of pulsed EUV radiation with different materials, further studies are focused on an optimization of both the achievable spatial resolution and the EUV energy density in the image plane of the Schwarzschild objective.

ACKNOWLEDGMENTS

The authors would like to thank the Bundesministerium für Bildung und Forschung for financial support within the project “KOMPASS” (Kompakte Strahlquelle hoher Brillanz für den weichen Röntgen-Spektralbereich). The cooperation with Dr. T. Waak/Jenoptik AG (Jena/Germany) is gratefully acknowledged, who performed the characterization of the EUV mirror substrates.

¹ See, e.g., *SPIE Microlithography 2005 Conference*, San Jose, California, 27 February–4 March 2005 (unpublished).

² U. Stamm, *J. Phys. D* **37**, 3244 (2004).

³ V. Banine and R. Moors, *J. Phys. D* **37**, 3207 (2004).

⁴ G. Baldacchini, S. Bollanti *et al.*, *IEEE J. Sel. Top. Quantum Electron.* **10**, 1435 (2004).

⁵ G. Baldacchini, F. Bonfigli *et al.*, *Radiat. Eff. Defects Solids* **157**, 569 (2002).

⁶ F. Bonfigli, A. Ya. Faenov, F. Flora *et al.*, *Phys. Status Solidi A* **202**, 250 (2005).

⁷ H. Gu and L. Qi, *Opt. Commun.* **210**, 299 (2002).

⁸ H. Gu and H. Liu, *Opt. Commun.* **201**, 113 (2002).

⁹ E. J. Caine and S. D. Miller, *J. Vac. Sci. Technol. B* **16**, 3232 (1998).

¹⁰ G. Baldacchini, F. Bonfigli *et al.*, *J. Nanosci. Nanotechnol.* **3**, 483 (2003).

¹¹ L. Juha, J. Krasa *et al.*, *Surf. Rev. Lett.* **9**, 347 (2002).

¹² S. Kranzusch and K. Mann, *Opt. Commun.* **200**, 223 (2001).

¹³ C. Peth, S. Kranzusch, K. Mann, and W. Viöl, *Rev. Sci. Instrum.* **75**, 3288 (2004).

¹⁴ S. Kranzusch, C. Peth, and K. Mann, *Rev. Sci. Instrum.* **74**, 969 (2003).

¹⁵ N. Benoit, S. Yulin, T. Feigl, and N. Kaiser, *Physica B* **357**, 222 (2005).

¹⁶ B. Schäfer and K. Mann, *Appl. Opt.* **41**, 2809 (2002).

¹⁷ B. Schäfer and K. Mann, *Rev. Sci. Instrum.* **71**, 2663 (2000).

¹⁸ Oliver Lammel, Thesis, University of Regensburg, 2002.

¹⁹ R. M. Montoreali, *Radiat. Eff. Defects Solids* **157**, 545 (2002).

²⁰ J. Nahum and D. A. Wiegand, *Phys. Rev.* **154**, 817 (1967).